Bioorganic Chemistry 93 (2019) 103286

Contents lists available at ScienceDirect

Bioorganic Chemistry

journal homepage: www.elsevier.com/locate/bioorg

Ebselen bearing polar functionality: Identification of potent antibacterial agents against multidrug-resistant Gram-negative bacteria

Cheng Chen, Kewu Yang*

Key Laboratory of Synthetic and Natural Functional Molecule Chemistry of Ministry of Education, Chemical Biology Innovation Laboratory, College of Chemistry and Materials Science, Northwest University, 1 Xuefu Avenue, Xi'an 710127, PR China

ARTICLE INFO

Keywords:
Gram-negative pathogens
Drug discovery
Ebselen analogues
Antibacterial activity

ABSTRACT

Antibiotic-resistant bacteria has become one of the greatest challenges to global human health today. Innovative strategies are needed to identify new therapeutic leads to tackle infections of drug-resistant Gram-negative bacteria. We herein synthesize a series of EB analogues to investigate their antibacterial activities. Select polar functionality at N-terminus of EB exhibited higher activities against multi-drug-resistant Gram-negative pathogens, including *E. coli*, *P. aeruginosa* and *K. pneumoniae*. EB analogue **4g** and **4i** exhibited potent antibacterial activities against *E. coli*-ESBL (MIC = 1–4 μg/mL) and *E. coli* producing NDM-1 (MIC = 4–32 μg/mL), which is superior to the traditional antibiotics (cefazolin, imipenem). Furthermore, the time-kill kinetics studies and the inhibition zone tests indicated that analogue **4i** effectively and rapidly cause death of *E. coli*-ESBL and *E. coli*-NDM-1. Additionally, accumulation assays and SEM images showed that **4i** could permeate bacterial membranes, leading to an irregular cell morphology. Importantly, bacterial resistance for analogue **4i** was difficult to induce against *E. coli*-ESBL. EB analogues here reported low cytotoxicity against L-929 cells and mice model *in vivo*. We believe that EB analogues with polar functionality could play a pivotal role in the development of novel antibacterial agents in eradicating multi-drug-resistant Gram-negative pathogens infections.

1. Introduction

The continuing and increasing prevalence of multidrug-resistant (MDR) Gram-negative bacteria (GNB) has become a tremendous threat to public health worldwide, these bacteria, including *Klebsiella pneumoniae, Pseudomonas aeruginosa, Acinetobacter baumannii and Escherichia coli*, are called antibiotic-resistant "priority pathogens" released by World Health Organization (WHO) in 2017 [1–3]. The dissemination of Extended Spectrum Beta-Lactamases (ESBL)-producing organisms and Carbapenem-resistant *Enterobacteriaceae* (CRE) are the major causes of healthcare-associated bacterial infection, such as those in the surgical site, urinary tract, intra-abdominal and bloodstream region [4,5]. In particular, CRE involves the most worrisome evolution of the antibiotic resistance crisis, which is almost resistant to all available antibiotics [6,7]. Currently, the clinically most important carbapenemases in *Enterobacteriaceae* consist of the class A enzymes of the *K. pneumoniae* carbapenemases (KPC) type, the zinc-dependent class B metallo-β-lactamases (MβLs) of the VIM, IMP, and NDM types and class D carbapenemases of the OXA-48 type [8,9]. These types of CRE are structurally and mechanistically different from each other, making it challenging to identify the antibacterial agent that is active against all types of CRE [10].

Gram-negative bacteria (GNB) have two cellular membranes, and the lipopolysaccharide-coated outer membrane impermeable to most small molecules is one of the largest of challenges in the discovery of new Gram-negative antibacterial agents [3,11]. In addition, there is a limited understanding of this type of compounds that can be accumulated in Gram-negative pathogens. One useful strategy for identifying the novel antimicrobials is to carefully monitor and tune these physicochemical properties of small-molecule that increase accumulation in GNB and enable broad antibacterial coverage [12]. The "eNTRy rules" reported by Richter et al showed the ability of diverse compounds to accumulate in *E. coli* led to the development of predictive guidelines for compound accumulation, which suggested that compounds are most likely to accumulate if they contain a primary amine, low globularity and relatively rigid. These guidelines were then successfully applied to convert a natural product that is active only against Gram-positive bacteria, into an antibiotic with activity against multi-drug-resistant Gram-negative pathogens [13].

In previous disclosures, Ebselen (EB) has antioxidant, anti-inflammatory and cytoprotective properties, and the safety of EB in humans has been demonstrated by three different clinical trials

* Corresponding author.
E-mail address: kwyang@nwu.edu.cn (K. Yang).

https://doi.org/10.1016/j.bioorg.2019.103286
Received 25 April 2019; Received in revised form 20 August 2019; Accepted 15 September 2019
Available online 16 September 2019
0045-2068/

investigating the treatment of stroke patients [14–16]. Moreover, EB has been shown to have excellent antimicrobial activity against clinical multidrug-resistant Gram-positive pathogens, including Methicillin-resistant *S. aureus* (MRSA) and Vancomycin-resistant *Enterococcus faecium* (VRE) [17]. Lu et al. revealed that EB, a substrate of mammalian thioredoxin reductase (TrxR) but an irreversible inhibitor of bacterial TrxR, blocks the electron transfer via TrxR and displays selectively antibacterial activity toward GSH-negative bacteria, with no inhibitory effect on GSH-positive bacteria, for example, *Escherichia coli* [18]. Additionally, Chiou et al and our previous studies showed that EB is a potent covalent inhibitor of NDM-1 binding the Cys208 at active site of enzyme, in combination β-lactams to combat effectively clinically isolates producing NDM-1 [8,19]. Ngo et al also reported that EB and its sulfur analogues (Ebsulfur) showed potent antibacterial efficacy against MRSA and also exhibited broad-spectrum antifungal activity [20,21]. However, EB did not show potent antimicrobial activity against Gram-negative pathogens, which might be due to its reduced ability to cross outer membrane barrier or the efflux pump rather than lack of target of EB inside Gram-negative bacteria [22]. Inspired by the above information, we herein synthesized a series of EB-based analogues appending various polar functionality at the N-terminus to further investigate antibacterial activities of these EB analogues in fighting against some of the most problematic Gram-negative bacteria in the clinic.

2. Results and discussion

2.1. Chemistry

To gain insights into the relationship that exists between physicochemical properties and antibacterial activity against GNB, we targeted the N-terminus of the EB scaffold for optimization through the incorporation of polar functionality with the goal of increasing accumulation of new EB small molecules. We initiated this study with a series of amidation for 2-(chloranylidene)-selanyl)benzoyl chloride (**3**) using small, different polar amines (Scheme 1). The synthetic procedure involved preparation of acyl chloride through reflux of disselenide and $SOCl_2$ at 85 °C and recrystallization using cyclohexane, then acyl chloride was dropwise added to solution of the appropriate amine and trimethylamine (TEA) at 0 °C to furnish the desired amidation product. Through this procedure, we synthesized Ebselen 4a and eight EB analogues **4b-g** in 56–75% yield (Scheme 1). Analogues **4e** and **4f** with Boc-group were deprotected using hydrochloric acid in methanol to afford **4h** (86% yield) and **4i** (92% yield), respectively. Ebselen and eight EB analogues we reported here had ClogP values with a range of 1.16–4.41, all EBs synthesized were advanced to antibacterial investigation.

2.2. Antimicrobial activity evaluation

Following chemical synthesis of these EB analogues bearing polarity at the *N*-terminus, EB **4a-i** were firstly assayed for antibacterial activities against Gram-positive strains: *S. aureus*, methicillin-resistant *S. aureus* (MRSA) and vancomycin-resistant *E. faecium* (VRE). Antibacterial activity was determined via microdilution minimum inhibitory concentration (MIC) assays that were performed in 96-well plates [23]. The tested compounds were screened in MIC assays using 2-fold serial dilutions (0.125 to 128 μg/mL) in three independent experiments. MIC data (Table 1) indicated that the EB analogues display 4–32-fold stronger antibacterial effect than the vancomycin as control (MIC = 2–256 μg/mL) on three Gram-positive strains tested, with an MIC value ranging from 0.25 to 64 μg/mL, the data previously reported also indicated EB against *S. aureus* ATCC strains with a MIC range of 0.125–7.8 μg/mL [17,20,22], and **4g** and **4i** were found to be the most potent compounds (MIC = 0.25–16 μg/mL). More importantly, both **4g** and **4i** with ClogP reducing appendage exhibited higher antibacterial property than the control (EB, **4a**).

Subsequently, to further investigate whether EB analogues with various polarity enhanced antibacterial activities against multi-drug-resistant Gram-negative strains, five clinical isolates Extended Spectrum Beta-Lactamases *E. coli* (*E. coli*-ESBL), Extended Spectrum Beta-Lactamases *K. pneumonia* (*K. pneumonia*-ESBL), *P. aeruginosa* and

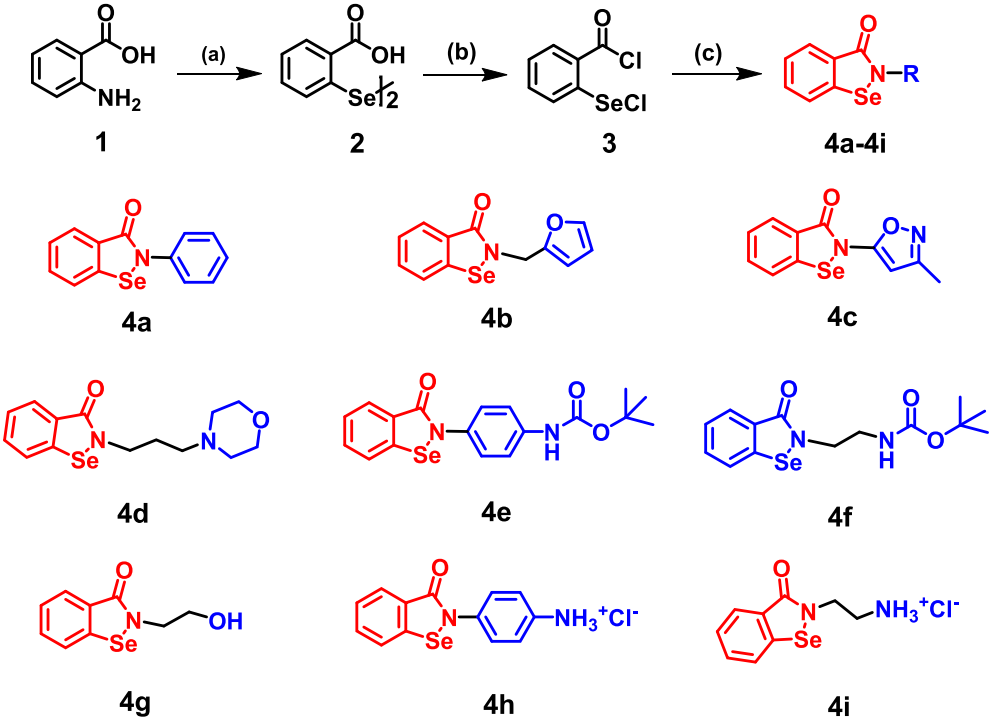

Scheme 1. Synthetic route and structures of EB analogues. Reagents and conditions: (a) (1) $NaNO_2$, HCl (aq), 0 °C, 30 min; (2) Na_2Se_2, H_2O, 0–60 °C, 6 h; (b) $SOCl_2$, DMF, reflux 3 h; (c) amine (excess)/TEA.

Table 1
MICs (μg/mL) of EB **4a** and analogues **4b-i** against multi-drug-resistant Gram-positive and Gram-negative bacteria, using vancomycin (Van) and cefazolin (Czo) as control.

	Strains	4a	4b	4c	4d	4e	4f	4g	4h	4i	Van	Czo
	ClogP[a]	3.7	2.9	1.95	2.3	4.41	3.04	1.16	2.37	1.27	–	–
G+	*S. aureus*	0.5	0.5	0.25	0.25	1	2	0.25	1	0.25	2	–
	MRSA	64	64	64	32	64	64	8	32	4	128	–
	VRE	64	64	32	64	64	64	16	32	8	256	–
G–	*E. coli*-ESBL[a]	> 128	> 128	64	64	> 128	> 128	4	> 128	2	–	512
	E. coli-ESBL[b]	> 128	> 128	64	> 64	> 128	> 128	4	> 256	1	–	256
	K. pneumonia-ESBL	> 128	> 128	> 64	64	> 128	> 64	8	> 128	4	–	256
	K. pneumonia-NDM-1	> 128	> 128	> 128	> 128	> 128	> 128	32	> 128	16	–	512
	P. aerugions	> 128	> 128	> 128	> 128	> 128	> 128	64	> 128	16	–	512

Notes: all the clinical isolates MRSA, VRE, *E. coli*-ESBL[a, b], *K. pneumonia*-ESBL, *K. pneumonia*-NDM-1, *P. aerugions* from the Health Science Center at Xi'an Jiaotong University China. All these isolates were identified by VITEK2 Compact (bioMérieux, France) and 16S rRNA gene sequencing. PCR and nucleotide sequencing were employed to screen for the presence of NDM genes. a: all ClogP calculated from ChemBioDraw Ultra 14.0. G+: Gram-positive bacteria, G−: Gram-negative bacteria.

Table 2
Antibacterial activities (MIC, μg/mL) of EB **4a** and analogues **4b-i**, cefazolin (Czo) and imipenem (IMI) against clinical isolates EC01-EC24 (*E. coli* producing NDM-1) and *E. coli* expressing MβLs.

Strains	4a	4b	4c	4d	4e	4f	4g	4h	4i	Czo	IMI
EC01	> 128	> 128	128	128	> 128	> 128	32	> 128	8	5000	128
EC04	> 128	> 128	64	128	> 128	> 128	16	128	16	100,000	64
EC06	> 128	> 128	> 128	> 64	> 128	> 128	16	> 128	4	2500	64
EC07	> 128	> 128	> 64	64	> 128	> 128	16	> 128	32	5000	128
EC08	> 128	> 128	128	64	> 128	128	8	> 128	4	10,000	128
EC10	> 128	> 128	128	> 128	> 128	> 128	32	> 128	32	2500	256
EC23	> 128	> 128	64	> 128	> 128	> 128	8	> 128	16	10,000	64
EC24	> 128	> 128	> 128	64	> 128	> 128	4	> 128	8	5000	64
E. coli-NDM-1	> 64	> 64	> 64	> 64	> 64	> 64	4	> 64	1	256	128
E. coli-CcrA	> 64	> 64	> 64	> 64	> 64	> 64	4	> 64	1	128	64
E. coli-VIM-2	> 64	> 64	> 64	> 64	> 64	> 64	2	> 64	1	256	128
E. coli-IMP-1	> 64	> 64	> 64	> 64	> 64	> 64	2	> 128	0.5	128	64
E. coli-ImiS	> 64	> 64	> 64	> 64	> 64	> 64	2	> 128	1	–	128
E. coli-L1	> 64	> 64	> 64	> 64	> 64	> 64	2	> 64	0.5	64	32

Notes: all the clinical isolates *E. coli* producing NDM-1 (EC01-24) from the Health Science Center at Xi'an Jiaotong University, China.

K. pneumonia-NDM-1 were used for evaluation of the EB analogues. MIC data (Table 1) showed that the **4g** and **4i** had the lowest ClogP (1.16 and 1.27), and both compounds were found to be effectively inactive against all Gram-negative strains tested with a MIC range of 1–64 μg/mL. Particularly, for *E. coli*-ESBL, **4i** proved to be the best MIC value of 1 μg/mL, being 256-fold more potent than the antibiotic cefazolin (MIC = 256 μg/mL). Nevertheless, for the other EB analogues with different ClogP values, the enhanced antibacterial activities against Gram-negative bacteria were not to be observed. Additionally, a comparison of Clog P for all EB analogues indicates that antibacterial activity increased with increased polarity attached to the *N*-terminus of EB (Fig. S1). We then assayed the antibacterial activity of the EB analogues against clinical isolates *E. coli* producing NDM-1 (EC01-EC24) and other five *E. coli* expressing MβLs, indicating that **4i** with low globularity, relatively rigid (rotatable bonds = 3), and primary amine showed strong antibacterial effect against clinically isolates and *E. coli* expressing MβLs, with a best MIC value of 4 μg/mL and 0.5 μg/mL for EC08, and *E. coli* expressing IMP-1 (Table 2), which are 256–2500-fold higher efficiency than the cefazolin (10000 μg/mL) and imipenem (128 μg/mL). The $MIC_{50/90}$ value for **4i** against all Gram-negative pathogens tested were 2.56 and 16.32 μg/mL, respectively. However, **4h** did not present antibacterial activity towards Gram-negative bacteria (GNB), probably because **4h** with sterically encumbered primary amine is not high accumulators, which is not in line with the eNTRy rules [13]. Additionally, MH buffer (pH ~ 7.4) was used in antibacterial assays, **4h** (pKa ~ 5) may exist in the uncharged form, so as to decrease accumulation on the surface.

2.3. Uptake of EB analogues by ESBL-E. coli

To investigate the uptake of EB analogues by ESBL-*E. coli* cells, ICP-AES (inductively coupled plasma absorbance emission spectroscopy) studies were carried out. Experiments to investigate the accumulation of selenium (Se) in the ESBL-*E. coli* were conducted at high concentrations. As shown in Fig. 1, accumulation of **4g** and **4i** uptake to 8×10^{-8} μg per cell about 2 h, which is obvious higher than other analogues. The presence of a primary amine or polar group is clearly important for accumulation in *E. coli*. The above accumulation results are consistent with their antibacterial activity.

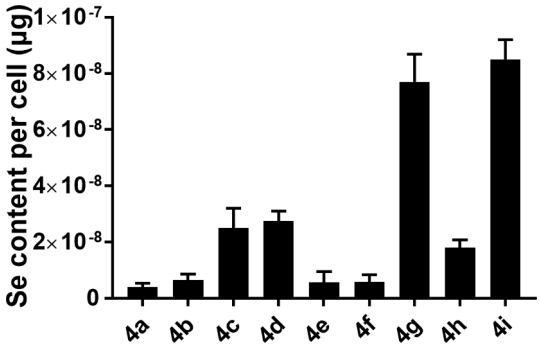

Fig. 1. ICP-AES data for the uptake of Se by ESBL-*E. coli* after exposure to different EB analogues. Se contents per cell are expressed as Se (μg) per cell.

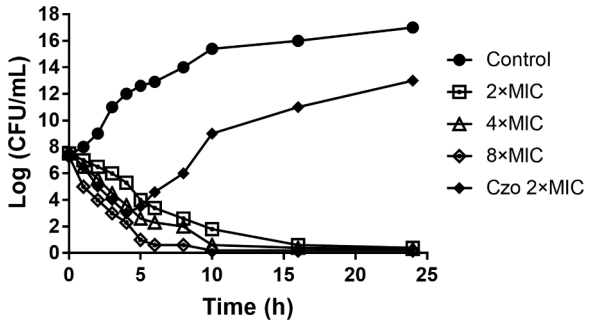

Fig. 2. Time-dependent killing curves. *E. coli*-ESBL were grown to early exponential phase and challenged with **4i** at 2 × MIC, 4 × MIC and 8 × MIC, and cefazolin (Czo) at 2 × MIC.

2.4. Time-dependent killing

To determine the bactericidal rate of EB analogues against Gram-negative bacteria, the time-kill kinetics of analogue **4i** was performed [24]. *E. coli*-ESBL and EC08 were grown to early exponential phase and challenged with **4i** (2×, 4×, 8 × MIC), and cefazolin (2 × MIC). As shown in Figs. 2 and S2, 4i had excellent bactericidal activity against *E. coli*-ESBL and EC08, showing superior activity compared with that of cefazolin in killing early exponential phase populations. Moreover, **4i** (8 × MIC) killed early exponential phase *E. coli*-ESBL and EC08 at 6 h, whereas cefazolin (2 × MIC) did not kill *E. coli*-ESBL and EC08 at 24 h. The cefazolin samples were cloudy after 10 h treatment, but the both samples treated with **4i** were clear (Fig. S3). These results suggest that **4i** rapidly kills both *E. coli*-ESBL and *E. coli* producing NDM-1.

2.5. Zeta potential (ζ) measurement

To obtain deeper insights into the interactions between EB analogues and *E. coli*-ESBL, Zeta potential (ζ) was employed to this study [25]. As shown in Fig. 3, after incubation with all analogues, only the ζ potential of *E. coli*-ESBL by treated with analogue **4h** and **4i** became more positive compared with other EB analogues. Clearly, the interaction of **4h** and **4i** with *E. coli*-ESBL was influenced obviously by the ionic strength, indicating that the accumulation of **4h** and **4i** to *E. coli*-ESBL was dominated by electrostatic interactions. **4i** showed the electrostatic interactions with negatively charged lipopolysaccharide of an outer membrane, so as to promote the accumulation of it on the cell surface and then enter into cell through bacterial porins. Though **4h** also accumulates on the surface of cell by electrostatic interactions, and make zeta potential of cell became more positive, it is difficult to cross the porins due to sterically encumbered primary amine, and could not exhibit antibacterial activity.

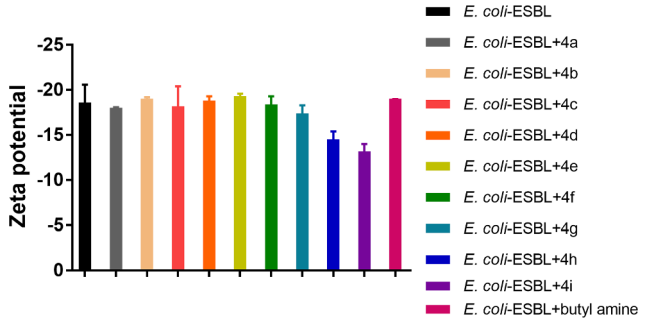

Fig. 3. Zeta potentials (ζ) of *E. coli*-ESBL in the absence and presence of all EB analogue, final measurements were performed in 1 mM PBS solution at 25 °C.

2.6. Inhibition zone tests

Thenceforward, to further elucidate the antibacterial effect of **4i** against different Gram-negative bacteria including: *E. coli* producing NDM-1, *E. coli*-ESBL, *P. aeruginosa* and *K. Pneumoniae-NDM-1*, the inhibition zone tests were carried out [26]. As shown in Fig. S4, there are gradually increasing diameter of inhibition zones for the antibacterial test with the concentration of **4i** raising. It clearly demonstrated that the introduction of a primary amine makes EB analogue **4i** had excellent antibacterial properties against the multidrug-resistant Gram-negative bacteria.

2.7. SEM characterization

We next advanced to be direct visualization of the morphological changes of bacteria in the presence of EB analogues using field-emission SEM [27,28]. As shown in Fig. 4, the control group exhibited a smooth cell surface and clear bacterial edges. After treatment with **4i**, catastrophic structural damages to the *E. coli*-ESBL and *P. aeruginosa* were visualized, and almost all the bacteria were collapsed and fused. SEM images showed an irregular cell morphology caused by **4i** possibly through permeabilizing bacterial membranes and then targeting related sulfhydryl-dependent enzymes of thioredoxin system in bacteria [29]. These results were consistent with antibacterial experiments.

2.8. Bacterial resistance studies

Subsequently, we evaluate the ability of analogue **4i** to suppress the development of resistance against Gram-negative *E. coli*-ESBL through resistance selection studies after a prolonged passage at sub-inhibitory concentrations. The control antibiotic cefazolin (Czo) was chosen for *E. coli*-ESBL. Only a 2-fold change was detected in the MIC of **4i** against *E. coli*-ESBL after 20 passages. However, antibiotic Czo displayed a 64-folds increase in the MIC (Fig. 5). These results indicated that analogue **4i** had major advantages compared to conventional antibiotic and induced less bacterial resistance.

2.9. Cytotoxicity assays

The potential toxicity of candidates is a major concern for development of clinically useful of broad-spectrum antibacterial agents. To verify the safety of EB analogues, analogue **4g** and **4i** were selected to a cytotoxicity assay with L929 cells at various concentrations (3.5, 7, 14, 28, 56, 112 μg/mL) [30]. As shown in Fig. 6, both compounds exhibited relatively low cytotoxicity against L929 cell, with a cell viability of 70% or higher at a concentration up to 28 μg/mL, which is higher than the effective antibacterial concentration. Furthermore, the median lethal dose (LD_{50}), a helpful pointer of the substance's acute toxicity, was established after intraperitoneal injection in Kunming mice 20–22 g followed by an observation period of 72 h. The LD_{50} values in mice was determined to be 61 mg/kg for **4i** (Fig. 7), suggesting a relatively low toxicity of EB analogue **4i** *in vitro* and *in vivo*.

3. Conclusions

In summary, a series of EB analogues **4a-i** with various polarity were synthesized and evaluated. Analogue **4g** and **4i**, with the lowest ClogP (1.16 and 1.27), were found to have excellent antibacterial activity against the multidrug-resistant Gram-negative bacteria, particularly *E. coli*-ESBL (MIC = 1–4 μg/mL) and carbapenem-resistant pathogens *E. coli* producing NDM-1 (MIC = 4–32 μg/mL), being more potent than the traditional antibiotics (cefazolin and imipenem). The $MIC_{50/90}$ values for **4i** against all Gram-negative pathogens tested was 2.56 and 16.32 μg/mL, respectively Furthermore, the time-kill kinetics studies, accumulation assays and SEM images revealed that the analogue **4i** could permeate bacterial membranes, leading to an irregular

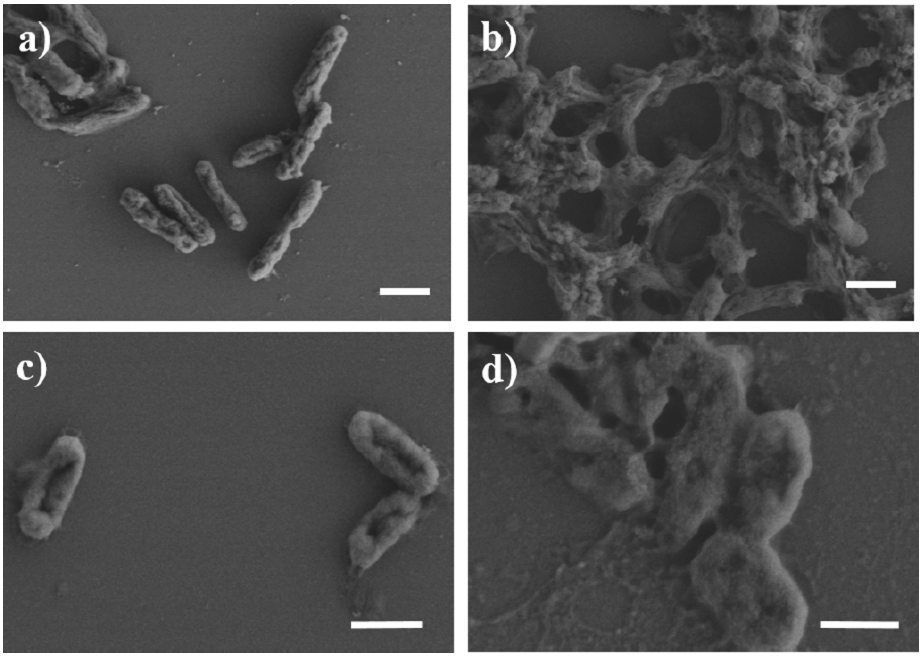

Fig. 4. SEM images of *E. coli*-ESBL and *P. aeruginosa* before (a, c) and after (b, d) treatment with analogue **4i**, bar scare: 5 μm.

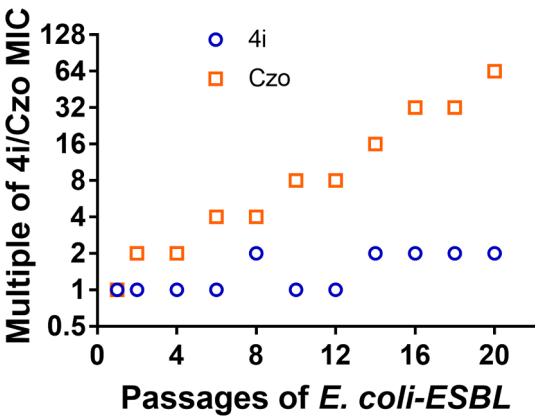

Fig. 5. Resistance acquisition curves during serial passage with the sub-inhibitory concentration of **4i** or Czo against *E. coli*-ESBL[b]. MIC test was performed every two passages.

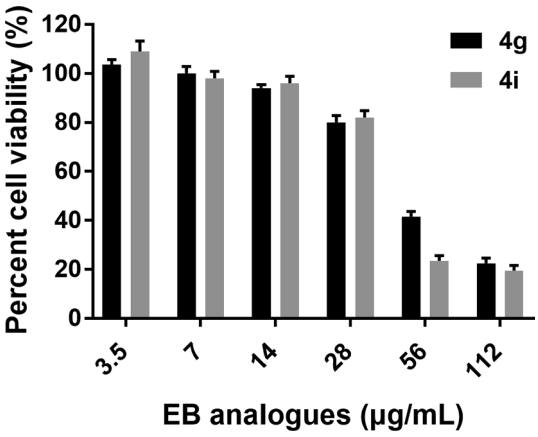

Fig. 6. Cytotoxicity assay in L929 cells were treated with EB analogues **4g** and **4i** at a concentration ranging from 3.5 to 112 μg/mL. DMSO was used as a negative control.

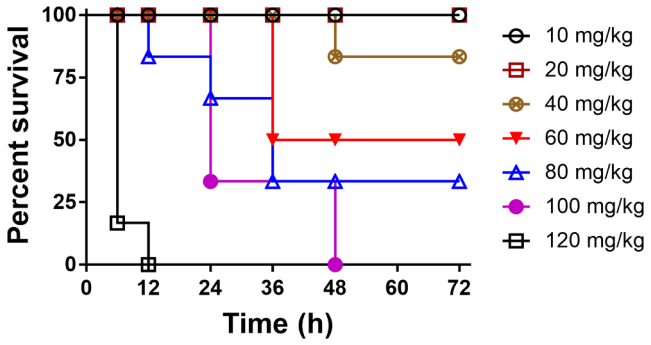

Fig. 7. Dose-response for EB analogue **4i** administrated by intraperitoneal injection (i.p.) route mice were observed up to 72 h (n = 6 per group).

cell morphology and rapid death of *E. coli*-ESBL and *E. coli*-NDM-1. Moreover, EB analogues did not induce bacteria to develop resistance. Also, EB analogues tested exhibited low cytotoxicity against L-929 cells and mice model *in vivo*. These studies demonstrated that the EB analogues with polarity present a novel scaffold for the development of antibacterial agents in combating multi-drug-resistant Gram-negative pathogens infections.

4. Material and methods

4.1. Chemistry

^{1}H and ^{13}C NMR spectra were recorded on a Bruker Avance III 400-MHz spectrometer. Chemical shifts are given in parts per million (ppm) on the delta scale. The peak patterns are reported as singlet (s), doublet (d), triplet (t), quartet (q), doublet doublet (dd), and mul-tiplet (m). The spectra were recorded with TMS as internal standard. Coupling constants (J) were reported in Hertz (Hz). Mass spectra were obtained on a micro TOF-Q (BRUKER) mass spectrometer. The reactions were followed by thin-layer chromatography (TLC) on glass packed precoated silica gel plates and visualized in an iodine chamber or with a UV lamp. Flash column chromatography was performed using silica gel (200–300 mesh) purchased from Qingdao Haiyang Chemical Co. Ltd. Activity evaluation of inhibitors was performed on an Agilent 8453 UV–Vis

spectrometer.

A solution of 2-(chloroseleno)benzoyl chloride (1 mmol) in dry ether (10 mL) was added dropwise over 30 min to a stirred solution of the appropriate amine (1.2 mmol) and triethylamine (3.5 mmol) in dry DCM (10 mL) at 0 °C. The reaction mixture was stirred at room temperature overnight. The solvent was removed under reduced pressure and the residue was washed with water (20 mL), and extracted with DCM (3 × 10 mL). The combined organic extracts were dried over anhydrous $MgSO_4$, the solvent removed was under reduced pressure, and the crude product was purified by flash column chromatography on silica gel (eluents: 10–50% ethyl acetate in petroleum gradient) [31]. All EB analogues except 4c and 4e have been reported.

4.1.1. 2-Phenylbenzo[d][1,2]selenazol-3(2H)-one (4a)

Gray solid, yield 80%, ^{1}H NMR (400 MHz, DMSO-d_6) δ 8.26 (d, J = 8.0 Hz, 1H), 7.90 (d, J = 7.5 Hz, 1H), 7.68–7.60 (m, 3H), 7.49–7.42 (m, 3H), 7.26 (t, J = 7.3 Hz, 1H). ^{13}C NMR (101 MHz, DMSO-d_6) δ 165.42, 140.48, 139.73, 132.37, 129.59, 128.23, 126.75, 126.55, 126.04, 125.01, 121.08. HRMS (ESI): *m/z* Calcd for: $C_{13}H_9NOSe$ $[M+Na]^+$ 297.9747; found 297.9729.

4.1.2. 2-(furan-2-ylmethyl)Benzo[d][1,2]selenazol-3(2H)-one (4b)

White solid, yield 65%, ^{1}H NMR (400 MHz, DMSO-d_6) δ 8.01 (d, J = 8.0 Hz, 1H), 7.84 (d, J = 7.7 Hz, 1H), 7.65–7.57 (m, 2H), 7.42 (t, J = 7.3 Hz, 1H), 6.45–6.42 (m, 2H), 4.93 (s, 2H). ^{13}C NMR (101 MHz, DMSO-d_6) δ 166.65, 151.58, 143.75, 142.48, 139.74, 131.98, 128.26, 127.89, 126.16, 111.17, 109.26, 40.09. HRMS (ESI): *m/z* Calcd for: $C_{12}H_9NO_2Se$ $[M+Na]^+$ 301.9696; found 301.9646.

4.1.3. 2-(3-methylisoxazol-5-yl)Benzo[d][1,2]selenazol-3(2H)-one (4c)

White solid, yield 65%, ^{1}H NMR (400 MHz, DMSO-d_6) δ 8.09 (d, J = 8.0 Hz, 1H), 7.92 (d, J = 7.7 Hz, 1H), 7.72 (t, J = 8.3 Hz, 1H), 7.48 (t, J = 7.7 Hz, 1H), 7.01 (s, 1H), 2.44 (s, 3H). ^{13}C NMR (101 MHz, DMSO-d_6) δ 171.48, 165.97, 159.48, 139.76, 133.79, 128.28, 127.77, 126.85, 126.79, 96.12, 12.84. HRMS (ESI): *m/z* Calcd for: $C_{11}H_8N_2O_2Se$ $[M+Na]^+$ 302.9649; found 302.9639.

4.1.4. 2-(3-morpholinopropyl)Benzo[d][1,2]selenazol-3(2H)-one (4d)

White solid, yield 65%, ^{1}H NMR (400 MHz, Chloroform-*d*) δ 8.03 (d, J = 7.8 Hz, 1H), 7.65–7.55 (m, 2H), 7.42 (d, J = 8.1 Hz, 1H), 3.92 (t, J = 6.7 Hz, 2H), 3.73 (t, J = 4.7 Hz, 4H), 2.49–2.39 (m, 6H), 1.92 (m, 2H). ^{13}C NMR (101 MHz, Chloroform-*d*) δ 167.46, 138.10, 131.93, 128.42, 127.46, 126.06, 123.91, 66.88, 54.79, 53.35, 42.71, 26.59. HRMS (ESI): *m/z* Calcd for: $C_{14}H_{18}N_2O_2Se$ $[M+Na]^+$ 349.0431; found 349.0367.

4.1.5. Tert-butyl (4-(3-oxobenzo[d][1,2]selenazol-2(3H)-yl)phenyl) carbamate (4e)

Grey solid, yield 86%, ^{1}H NMR (400 MHz, DMSO-d_6) δ 8.15 (d, J = 8.0 Hz, 1H), 7.91–7.84 (m, 1H), 7.70–7.61 (m, 1H), 7.57–7.40 (m, 5H), 1.49 (s, 9H). ^{13}C NMR (101 MHz, DMSO-d_6) δ 165.33, 153.23, 139.53, 137.83, 134.22, 132.38, 129.07, 128.23, 126.58, 125.78, 118.99, 79.63, 28.59. HRMS (ESI): *m/z* Calcd for: $C_{18}H_{19}N_2O_3Se$ $[M+Na]^+$ 413.0380; found 413.0375.

4.1.6. Tert-butyl (2-(3-oxobenzo[d][1,2]selenazol-2(3H)-yl)ethyl) carbamate (4f)

White solid, yield 75%,^{1}H NMR (400 MHz, Chloroform-*d*) δ 8.03 (d, J = 7.8 Hz, 1H), 7.69 (d, J = 8.0 Hz, 1H), 7.58 (td, J = 7.7, 1.3 Hz, 1H), 7.45–7.38 (m, 1H), 3.95 (t, J = 5.7 Hz, 2H), 3.44 (q, J = 5.9 Hz, 2H), 1.41 (s, 9H). ^{13}C NMR (101 MHz, Chloroform-*d*) δ 170.11, 155.98, 138.40, 132.04, 128.67, 126.20, 124.29, 45.84, 28.38, 8.65. HRMS (ESI): *m/z* Calcd for: $C_{14}H_{19}N_2O_3Se$ $[M+H]^+$ 343.0561; found 343.0526.

4.1.7. 2-(2-hydroxyethyl)Benzo[d][1,2]selenazol-3(2H)-one (4g)

White solid, yield 62%, ^{1}H NMR (400 MHz, DMSO-d_6) δ 8.04 (d, J = 8.0 Hz, 1H), 7.82 (d, J = 7.7 Hz, 1H), 7.59 (t, J = 7.6 Hz, 1H), 7.40 (t, J = 7.3 Hz, 1H), 3.81 (t, J = 5.2 Hz, 2H), 3.63 (q, J = 5.1 Hz, 2H). ^{13}C NMR (101 MHz, DMSO-d_6) δ 167.06, 140.66, 131.77, 128.11, 127.64, 126.08, 126.01, 60.89, 46.56. HRMS (ESI): *m/z* Calcd for: $C_9H_9NO_2Se$ $[M-H]^-$ 241.9720; found 241.9768.

4.1.8. 2-(3-oxobenzo[d][1,2]selenazol-2(3H)-yl)ethan-1-aminium chloride (4h)

White solid, yield 86%. ^{1}H NMR (400 MHz, D_2O) δ 8.08 (d, J = 8.0 Hz, 1H), 7.94–7.86 (m, 2H), 7.73–7.67 (m, 2H), 7.49 (t, J = 7.5 Hz, 1H), 7.12 (d, J = 9.0 Hz, 2H). ^{13}C NMR (101 MHz, DMSO-d_6) δ 165.56, 140.91, 140.26, 132.07, 130.09, 128.53, 127.99, 127.50, 126.34, 125.67, 124.46. HRMS (ESI): *m/z* Calcd for: $C_{13}H_{11}N_2OSe$ $[M+H]^+$ 291.0031; found 291.0060.

4.1.9. 4-(3-oxobenzo[d][1,2]selenazol-2(3H)-yl)benzenaminium chloride (4i)

White solid, yield 92%. ^{1}H NMR (400 MHz, D_2O) δ 7.84 (t, J = 8.7 Hz, 1H), 7.68–7.59 (m, 2H), 7.48–7.41 (m, 1H), 4.08 (t, J = 5.8 Hz, 2H), 3.14 (q, J = 7.3 Hz, 2H). ^{13}C NMR (101 MHz, D_2O) δ 169.59, 132.67, 128.24, 127.52, 126.46, 126.04, 124.81, 41.95, 39.48. HRMS (ESI): *m/z* Calcd for: $C_9H_{11}N_2OSe$ $[M+H]^+$ 243.0031; found 243.0042.

4.2. MIC determination

A single colony of clinical isolates *S. aureus*, MRSA, VRE, *E. coli*-ESBL, *P. aeruginosa*, *K. Pneumoniae* and *EC 01*-24 producing NDM-1 on LB agar plates was transferred to 5 mL of Mueller-Hinton (MH) liquid medium and grown at 37 °C overnight. The bacterial cells were collected by centrifugation (4000 rpm for 10 min). After discarding the supernatant, the pelleted cells were re-suspended in MH medium and diluted to an OD_{600} of 0.5. MIC values were determined by using the CLSI guidelines [32]. The MIC was interpreted as the lowest concentration of the drug that completely inhibited the visible growth of bacteria after incubating plates for at least 16 h at 37 °C. Each inhibitor was tested in triplicate.

4.3. Time-dependent killing

A single colony of clinical isolates *E. coli-ESBL* and EC08 on LB agar plates was transferred to 5 mL of Mueller-Hinton (MH) liquid medium and grown at 37 °C overnight. Bacteria were then treated with cefazolin (2 × MIC) and **4i** at 2×, 4×, 8 × MIC, respectively, in culture tubes at 37 °C, 225 rpm. At different times (0–24 h) intervals 20 μL of aliquots from the suspension was subjected to 10-fold serial dilution in 1 × PBS. 10 μL of the dilution was plated on solid agar plates and incubated at 37 °C for 16–18 h. The bacterial colonies were counted and results represented in log10 (CFU/mL) use the origin 8.0 [24].

4.4. Zeta potential measurements

The *E. coli* in PBS was incubated with 10 mM all EB analogue **4a-i** at 37 °C for 10 min. After that, the unbound compound was removed with centrifugation (8000 rpm for 5 min). The obtained pellets were washed with PBS solution, respectively. After centrifugation (8000 rpm for 5 min), the pellets were resuspended in 1 mL PBS and kept on ice. The specimens were prepared for zeta potential measurements. The *E. coli* incubated without EB analogues as the control group was conducted under the same condition.

4.5. Uptake of all EB analogues by ESBL-E. coli and determination of intracellular Se contents

Uptake and cellular accumulation of all EB analogues by ESBL-*E. coli* was determined by measuring bacterial cell Se content by ICP-AES as follows. ESBL-*E. coli* cultures were grown to OD_{600} = 1.0 in LB broth, washed in PBS, and then resuspended in PBS to approximately 10^8–10^9 CFU/mL. EB analogues **4a-i** was added to cells at 20 μM, and then 5 mL samples of culture were harvested at 60 min after EB analogues addition. The untreated cells were also taken for comparison. Samples were centrifuged for 20 min to obtain cell pellets to discard unbound extracellular EB analogues. To prepare cell material for ICP-AES, cell pellets were resuspended in 0.5 mL nitric acid (69% (w/v) and then placed in a sonicator bath for 30 min to completely dissolve cells. The resulting digest was then diluted to a final volume of 5 mL with diluted nitric acid, and then samples were analyzed on IRIS Advantage (Thermo Scientific) inductively-coupled plasma-atomic emission spectrophotometer. Levels of Se in the samples were determined by a calibration curve using multielement standard solutions containing 0.1, 0.2, 5 and 10 mg/L Se.

4.6. Inhibition zone tests

*EC*08 producing NDM-1, *E. coli*-ESBL, *P. aeruginosa* and *K. Pneumoniae*-NDM-1 was administered to the liquid medium, and cultured on it by air bath oscillator for 5 h. The rotating speed was 150 rpm, the temperature was 37 °C. Then, bacteria were vaccinated to solid medium. After drilling holes on the Agar plate using the oxford ring, and 10 μL the different concentration of compound **4i** (1–1024 μg/mL) was added, then developed under the incubator for 16–18 h at 37 °C and observed the bacteriostatic circle.

4.7. SEM characterization

To directly visualize the morphological changes of *E. coli*-ESBL and *P. aeruginosa* by compound **4i**, SEM characterization was employed to this study. After the operation according to antibacterial experiments, the mixture of cells and **4i** was centrifuged (3500*g* for 10 min). The supernatants were removed, and the bacterial pellets were fixed with 0.5% glutaraldehyde in PBS at room temperature for 30 min. Then, 2 μL aliquots of bacterial suspensions were transferred onto clean silicon slices. As soon as the specimens became dried, 0.1% glutaraldehyde was added for further fixation for 3 h. Next, the specimens were washed with sterile water twice and then dehydrated with increasing concentrations of ethanol (40% for 30 min, 70% for 30 min, 90% for 30 min, and 100% for 30 min). At last, the dried specimens were coated with platinum for SEM measurements.

4.8. Cytotoxicity assays

A cytotoxicity assay was performed to evaluate the toxicity of analogues **4g** and **4i** to mouse fibro-blast cells (L929). The cells were seeded into 96-well plates at cell density of 1.0×10^4 cells/well in 100 μL of culture medium and maintained for 24 h. Then solutions of compound **4g** and **4i** with different concentrations were added to 96-well plates respectively, and incubated for another 48 h. Six wells containing only cells suspended in a mixture of 99 μL of complete medium and 1 μL of DMSO were used as the control for investigating cell-viability. Six wells containing only the complete medium were used as the blank control. Following that, the medium was removed. Finally, 100 μL of fresh culture medium and 10 μL of Cell Counting Kit solution (purchased from 7Sea) were added to each well. After incubation for 4 h, the 96-well plates were then vigorously shaken to solubilize the formazan product and the absorbance at a wavelength of 450 nm was read on a Microplate Reader and analyzed. All experiments were conducted in triplicate.

4.9. Determination of median lethal dose (LD_{50})

Kunming mice weighing 20–22 g were obtained from Experimental Animal Center, Health Science Center of Xi'an Jiaotong University. The animals were kept in a room temperature. For each compound, the animals were randomly divided into 7 groups of 6 animals. Each group of animals are administrated different doses of compound tested (10–120 mg/kg). The animals were observed during 72 h after administering the test compound. The geographic mean of the least dose that killed mice (LD_{100}) and the highest dose that did not induced mortality (LD_0) was taken as the LD_{50}.

Acknowledgements

This work was supported by grants 21572179 (to K.W.Y.) from the National Natural Science Foundation of China.

Declaration of Competing Interest

None.

Appendix A. Supplementary material

Supplementary data to this article can be found online at https://doi.org/10.1016/j.bioorg.2019.103286.

References

[1] C.L. Ventola, The antibiotic resistance crisis: part 2: management strategies and new agents, P & T: Peer-Rev. J. Formul. Manage. 40 (2015) 344–352.
[2] L.B. Rice, Federal funding for the study of antimicrobial resistance in nosocomial pathogens: no ESKAPE, J. Infect. Dis. 197 (2008) 1079–1081.
[3] P.A. Smith, M.F.T. Koehler, H.S. Girgis, et al., Optimized arylomycins are a new class of Gram-negative antibiotics, Nature 561 (2018) 189–194.
[4] https://www.cdc.gov/drugresistance/threat-report-2013/pdf/ar-threars-2013-508.pdf.
[5] T.F. Durand-Reville, S. Guler, J. Comita-Prevoir, et al., ETX2514 is a broad-spectrum beta-lactamase inhibitor for the treatment of drug-resistant Gram-negative bacteria including Acinetobacter baumannii, Nat. Microbiol. 2 (2017) 17104–17133.
[6] A.C. Croft, A.V. D'Antoni, S.L. Terzulli, Update on the antibacterial resistance crisis, Med. Sci. Monitor Int. Med. J. Exp. Clin. Res. 13 (2007) 103–118.
[7] Y.J. Zhang, W.M. Wang, P. Oelschlaeger, et al., Real-time monitoring of NDM-1 activity in live bacterial cells by isothermal titration calorimetry: a new approach to measure inhibition of antibiotic-resistant bacteria, ACS Infect. Dis. 4 (2018) 1671–1678.
[8] C. Chen, Y. Xiang, K.-W. Yang, et al., A protein structure-guided covalent scaffold selectively targets the B1 and B2 subclass metallo-β-lactamases, Chem. Commun. 54 (2018) 4802–4805.
[9] L.S. Tzouvelekis, A. Markogiannakis, M. Psichogiou, et al., Carbapenemases in Klebsiella pneumoniae and other Enterobacteriaceae: an evolving crisis of global dimensions, Clin. Microbiol. Rev. 25 (2012) 682–700.
[10] X. Jiang, M.M.H. Ellabaan, P. Charusanti, et al., Dissemination of antibiotic resistance genes from antibiotic producers to pathogens, Nat. Commun. 8 (2017) 15784–15791.
[11] M.F. Richter, P.J. Hergenrother, The challenge of converting Gram-positive-only compounds into broad-spectrum antibiotics, Ann. N. Y. Acad. Sci. 1435 (2019) 18–38.
[12] D.G. Brown, T.L. Maydracka, M.M. Gagnon, et al., Trends and exceptions of physical properties on antibacterial activity for gram-positive and gram-negative pathogens, J. Med. Chem. 57 (2014) 10144–10161.
[13] M.F. Richter, B.S. Drown, A.P. Riley, et al., Predictive compound accumulation rules yield a broad-spectrum antibiotic, Nature 545 (2017) 299–304.
[14] M.J. Parnham, H. Sies, The early research and development of ebselen, Biochem. Pharmacol. 86 (2013) 1248–1253.
[15] G.K. Azad, R.S. Tomar, Ebselen, a promising antioxidant drug: mechanisms of action and targets of biological pathways, Mol. Biol. Rep. 41 (2014) 4865–4879.
[16] J. Kil, E. Lobarinas, C. Spankovich, et al., Safety and efficacy of ebselen for the prevention of noise-induced hearing loss: a randomised, double-blind, placebo-controlled, phase 2 trial, Lancet 390 (2017) 969–979.
[17] S. Thangamani, W. Younis, M.N. Seleem, Repurposing ebselen for treatment of multidrug-resistant staphylococcal infections, Sci. Rep. 5 (2015) 11596–11609.
[18] J. Lu, A. Vlamis-Gardikas, K. Kandasamy, et al., Inhibition of bacterial thioredoxin reductase: an antibiotic mechanism targeting bacteria lacking glutathione, FASEB J. 27 (2012) 1394–1403.
[19] J. Chiou, S. Wan, K.F. Chan, et al., Ebselen as a potent covalent inhibitor of New Delhi metallo-beta-lactamase (NDM-1), Chem. Commun. 51 (2015) 9543–9546.

[20] H.X. Ngo, S.K. Shrestha, K.D. Green, et al., Ebsulfur analogues as potent antibacterials against MRSA, Bioorg. Med. Chem. 24 (2016) 6298–6306.
[21] H.X. Ngo, S.K. Shrestha, S. Garneau-Tsodikova, Identification of ebsulfur analogues with broad-spectrum antifungal activity, ChemMedChem 11 (2016) 1507–1516.
[22] S. Thangamani, W. Younis, M.N. Seleem, Repurposing clinical molecule ebselen to combat drug resistant pathogens, PLoS ONE 10 (2015) e0133877.
[23] J.M. Andrews, Determination of minimum inhibitory concentrations, J. Antimicrob. Chemother. 49 (2001) 1049.
[24] W. Chu, Y. Yang, S. Qin, et al., Low-toxicity amphiphilic molecules linked by an aromatic nucleus show broad-spectrum antibacterial activity and low drug resistance, Chem. Commun. 55 (2019) 4307–4310.
[25] H. Sun, B. Yin, H. Ma, et al., Synthesis of a novel quinoline skeleton introduced cationic polyfluorene derivative for multimodal antimicrobial application, ACS Appl. Mater. Interf. 7 (2015) 25390–25395.
[26] P.Y. Bai, S.S. Qin, W.C. Chu, et al., Synthesis and antibacterial bioactivities of cationic deacetyl linezolid amphiphiles, Eur. J. Med. Chem. 155 (2018) 925–945.
[27] Y. Zhu, C. Xu, N. Zhang, et al., Polycationic synergistic antibacterial agents with multiple functional components for efficient anti-infective therapy, Adv. Funct. Mater. 28 (2018) 1706709–1706720.
[28] S. Zhu, X. Wang, Y. Yang, et al., Conjugated polymer with aggregation-directed intramolecular Förster resonance energy transfer enabling efficient discrimination and killing of microbial pathogens, Chem. Mater. 30 (2018) 3244–3253.
[29] L. Zou, J. Lu, J. Wang, et al., Synergistic antibacterial effect of silver and ebselen against multidrug-resistant Gram-negative bacterial infections, EMBO Mol. Med. 9 (2017) 1165–1178.
[30] C. Chen, Y. Xiang, K.W. Yang, et al., Mercaptoacetate thioesters and their hydrolysate mercaptoacetic acids jointly inhibit metallo-β-lactamase L1, Med. Chem. Comm 9 (2018) 1172–1177.
[31] K. Macegoniuk, E. Grela, J. Palus, et al., 1,2-Benzisoselenazol-3(2H)-one derivatives as a new class of bacterial urease inhibitors, J. Med. Chem. 59 (2016) 8125–8133.
[32] F.R. Cockerill, Methods for dilution antimicrobial susceptibility tests for bacteria that grow aerobically: approved standard-ninth edition, MO7-A9. Clinical and Laboratory Standards Institute, Wanye, PA, 2012.